Primitive Path Identification and Statistics in Molecular Dynamics Simulations of Entangled Polymer Melts

Qiang Zhou and Ronald G. Larson*

Department of Mechanical Engineering, University of Michigan, Ann Arbor, Michigan 48109-2036

Received February 17, 2005; Revised Manuscript Received April 13, 2005

ABSTRACT: To identify primitive paths, which are centerlines of confining tubes, two leading methods, namely total quadratic energy minimization and length minimization, are explored and compared in molecular dynamics (MD) simulations of linear pearl-necklace polymer chains. Energy minimization leads to a slightly larger averaged length but much narrower contour length distribution around the average length than does length minimization. Applications of both methods to melts of linear polymers in MD simulations confirm a quadratic entropic potential governing the primitive path length distribution. However, length minimization leads to a prefactor of around 1.5, in agreement with the classical result of Doi and Edwards, while energy minimization gives a prefactor of around 3.0.

I. Introduction

Identification of primitive paths in a well-equilibrated polymer melt is one of the major challenges in linking the widely used tube theory to molecular reality in entangled polymeric systems. While the "tube" represents a volume of space that can be explored by a chain without violating the topological constraints, the "primitive path", according to Edwards, is the shortest path the chain could take without violating these constraints. To extract the primitive path of a polymer chain in an entangled system, one could hypothetically fix one end of the polymer and "reel in" the polymer from the other end.[1] Rubinstein and Helfand[2] suggested that the least arbitrary way of identifying primitive paths is to reel in simultaneously and continuously all chains until no further loops can be removed. This procedure corresponds roughly to a total length minimization or, equivalently, a minimization of total "energy" with energy taken to be proportional to the total path length of all chains. Alternatively, primitive paths have been identified through minimization of the sum of energies over all springs that connect neighboring beads along the chain, where the spring energies are quadratic in the spring length for small spring extensions.[3,4] However, minimizing the quadratic spring energy could lead to a very different entanglement network than is obtained by minimizing the total length of all primitive paths.

In this paper, we explore the difference between identification of primitive paths by minimizing the total length vs minimizing total energy in large systems of entangled linear polymers. In the next section we briefly review the MD simulation method for pearl-necklace chains. Primitive path identification is explored in section III. We discuss and summarize the results in section IV and V.

II. Molecular Dynamics Simulation of the Pearl-Necklace Bead−Spring Model

In this work, polymers are represented by beads connected by short springs in a manner identical to that of Auhl et al.[5] The spring represents somewhat less than one Kuhn step of the polymer, depending on the bending potential used. Excluded-volume interactions are included through the repulsive Lennard-Jones potential:

$$U_{\mathrm{LJ}}(r) = \begin{cases} 4\epsilon\left\{(\sigma/r)^{12} - (\sigma/r)^6 + \frac{1}{4}\right\} & r \le r_c \\ 0 & r \ge r_c \end{cases}$$

where the cutoff distance $r_c = 2^{1/6}\sigma$ is chosen so that only the repulsive part of the Lennard-Jones potential is used. The energy scale is set by $\epsilon = k_B T$ and the length scale by σ, both of which are set to unity in our simulations. The constant term in the potential is added so that there is no discontinuity in total energy at the cutoff distance.

A finitely extensible nonlinear elastic (FENE) potential is used here to model the spring:

$$U_{\mathrm{FENE}}(r) = \begin{cases} -0.5kR_0^2 \ln(1 - (r/R_0)^2) & r \le R_0 \\ \infty & r \ge R_0 \end{cases}$$

The spring is made short and stiff enough so that there is not enough room between connected beads for another bead to pass between them. Thus, chain crossing is disallowed. We take the spring constant to be $k = 30\epsilon/\sigma^2$ and the maximum length of the spring to be $R_0 = 1.5\sigma$.

The MD method integrates an equation of motion, namely

$$\ddot{\mathbf{r}}_i = -\nabla U - \Gamma \dot{\mathbf{r}}_i + \mathbf{W}_i(t) \qquad (1)$$

where $\mathbf{r}_i$ is the position vector for bead i, and the potential U is comprised of the pairwise Lennard-Jones potential and the FENE potential.

The last two terms in eq 1 are not common in MD simulations developed for atomistic simulations. They are respectively an energy dissipation term due to friction of the bead with a hypothetic solvent and a thermal energy input term from the random thermal forces generated by that solvent. Γ is the friction coefficient of the bead with the solvent and is arbitrarily set to $0.5m/\tau$, where m is the mass unit and $\tau = \sigma(m/\epsilon)^{1/2}$ is the time unit. $\mathbf{W}_i$ is a Gaussian white noise, which is related to the friction coefficient by $\langle \mathbf{W}_i(t) \cdot \mathbf{W}_j(t') \rangle =$

10.1021/ma050347s CCC: $30.25
Published on Web 05/25/2005

$\delta_{ij}\delta(t - t')6k_BT\Gamma$. The fictitious solvent effects on the polymer dynamics are thus modeled by connecting the system to a solvent and friction heat bath, and the solvent molecules are not explicitly simulated. This method provides a convenient thermostat to regulate temperature and is appropriate for our bead−spring model, in which atomistic motions have been coarse-grained away.

We perform constant NVT simulations in a cubic simulation cell with periodic boundaries for monodisperse linear polymers with a monomer number density $\rho = 0.85\sigma^{-3}$. The average monomer length is $\langle b^2\rangle^{1/2} = 0.97\sigma$, which is the point at which a net zero force is produced by the sum of the Lennard-Jones repulsive potential and the FENE attractive potential between neighboring beads along the chain. Equation 1 is integrated using a velocity-Verlet method with a time step size $\Delta t = 0.012\tau$. Two systems are studied here: 1504×350 and 6016×350, where $M \times N$ represents a system with M chains, each chain containing N beads. Equilibrations of these systems are achieved following the slow push-off method by Auhl et al.[5] with improved initial configurations. A small system, 500×100, is first equilibrated through long MD simulations. Next, we pull out all the chains in the simulation box and cut them into halves to construct a database of "building blocks" for long chains. We then generate the initial configurations by randomly joining these building blocks into long chains with 350 beads.

III. Primitive Path Identification

As described by Doi and Edwards,[6] a polymer chain in a tube is subject to end-stretching tension because more freedom is available outside the tube than inside. On the other hand, a polymer chain tends to retract in the tube when stretched due to the entropic spring. As a result, polymer chains have a length distribution around a nonzero equilibration tube length L_{eq}. This distribution is essential to understanding the relaxation spectrum of polymer molecules with branched architectures. The distribution is usually written in the form of a potential

$$P(L) \simeq \exp\left[-\frac{U(L)}{k_BT}\right] \tag{2}$$

where $P(L)$ is the probability density function of the distribution of primitive path lengths and U is the potential governing fluctuations in primitive path length. In a straight rectangular confining tube,[6] a polymer chain with a quadratic spring potential and fixed end tension equal to $3k_BT/a$ where a is the tube diameter yields the frequently used quadratic potential governing fluctuations in the length of the primitive path: $U(L) = \nu k_BTZ(L/L_{eq} - 1)^2$, where $\nu = 1.5$, L_{eq} is the equilibrated or averaged primitive path length, and Z is the number of entanglements. However, theoretical predictions and simulations on simple lattices[2] have produced different potentials and very different prefactors, ν. A recent lattice simulation using the bond fluctuation model[7] by Shanbhag and Larson,[8] however, verified the quadratic form and the $\nu = 1.5$ prefactor. Nevertheless, what is still lacking is a determination of the fluctuation potential using a real-space simulation.

The fast and accurate equilibration method by Auhl et al.[5] enabled the identification of the primitive paths in small systems by Everaers et al.[3] In this method, one fixes the ends of all polymer chains in an equilibrated polymer melt and disables the excluded-volume interactions between neighboring beads along each chain while retaining repulsion between beads on different chains and dropping the temperature slowly to zero. Without local excluded-volume interactions along the chain, the polymer chain shrinks in length in this cooling procedure but cannot pass through neighboring chains and so tends toward the shortest path that does not violate topological interactions with other chains. Primitive paths are then obtained by minimizing the total energy of the system, which mainly consists of the quadratic spring energy along the chain. Because the interchain excluded volume is maintained to prevent chain crossing, this procedure leads to primitive paths with finite thickness. This is not a serious problem because the thickness of the primitive path is just the bead diameter, which is small compared to the effective random walk step length of the tube. However, this method of primitive path identification assigns a quadratic energy to the primitive paths, which does not have a clear physical justification. A primitive path, unlike an entropic spring of the polymer chain, has no entropic energy along its contour; rather, it is an instantaneous contour of the topological constraints enforced by surrounding chains. So any tension along the primitive path is not physically motivated but has a dramatic influence on the distributions of primitive paths. However, we do need some chain tension to shrink the chain length in the cooling procedure toward a well-defined "minimal" path. An alternative chain tension that we can introduce during the cooling procedure might be to use a small constant force for all the chains regardless of their lengths. A cooling procedure with constant spring force corresponds to a minimization of the total length of all primitive paths.

Table 1. Numbers of Entanglements, Standard Deviations, and Primitive Path Distribution Exponents Obtained Using the Potential in Eq 3 with Various Truncation Distances ($M \times N = 1504 \times 350$)

	$r_{tr} = 0.0\sigma$	$r_{tr} = 0.1\sigma$	$r_{tr} = 0.2\sigma$	$r_{tr} = 0.3\sigma$	$r_{tr} = 0.4\sigma$
Z	5.14 ± 0.06	5.13 ± 0.07	5.05 ± 0.08	5.01 ± 0.09	5.01 ± 0.09
$\bar{\sigma}$	0.84	0.92	1.19	1.26	1.26
ν	3.06 ± 0.18	3.11 ± 0.12	1.94 ± 0.12	1.60 ± 0.14	1.53 ± 0.10

To implement the length minimization method for finding primitive paths, one can assign a constant spring force to all polymer chains, but otherwise use the cooling procedure of Everaers et al.[3] However, a finitely extensible nonlinear elastic (FENE) spring with a force that becomes singular at finite extension is essential to preserve the topology of the system and prevent beads of one chain from fitting between neighboring beads of a second chain. Therefore, we use a truncated FENE spring potential during the cooling process as follows:

$$U_{trFENE}(r) = \begin{cases} (r - r_{tr})U'_{FENE}(r_{tr}) + U_{FENE}(r_{tr}) & r < r_{tr} \\ U_{FENE}(r) & r \geq r_{tr} \end{cases} \tag{3}$$

where r_{tr} is the location of the truncation. According to this potential, the spring force is constant for distances $r < r_{tr}$ and reverts to a FENE spring force for $r \geq r_{tr}$. With this spring law, we can smoothly switch from energy minimization to length minimization by increasing r_{tr} from zero. Table 1 shows the results of simulations with 1504 chains, each of which has 350 beads. These chains are long enough to be in the well-entangled

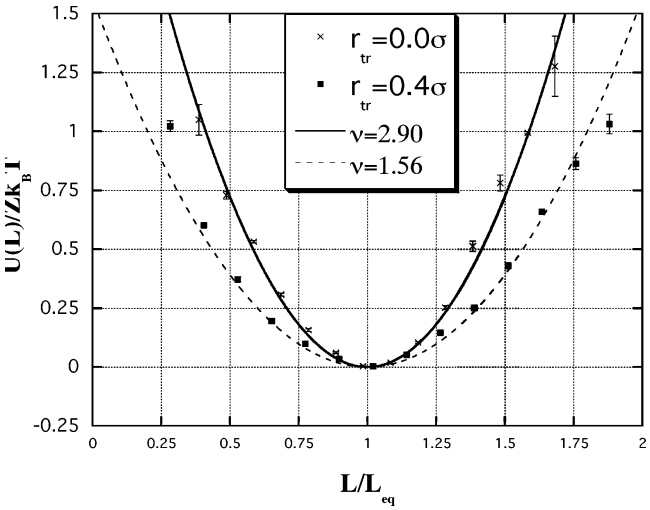

Figure 1. Potentials of primitive path distributions in a system of 6016 chains, each of which has 350 beads. Potentials are obtained through energy minimization, $r_{tr} = 0.0\sigma$, and length minimization, $r_{tr} = 0.4\sigma$. Here $U(L)/k_BT = \ln(P(L))$, where $P(L)$ is the distribution of primitive path lengths.

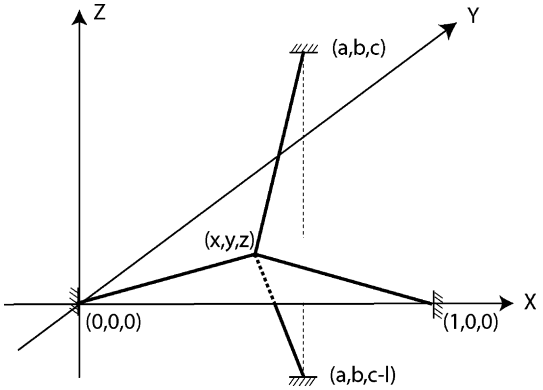

Figure 2. Two orthogonal chains with a single entanglement point.

region.[9−13] As the constant force region in the truncated FENE spring is enlarged beyond $r_{tr} = 0.2\sigma$, the distribution of primitive path lengths broadens, as shown by the increase in the standard deviation, $\bar{\sigma}$. As r_{tr} increases, the average number of entanglements does not change very much, but there is a decrease in the value of ν, the coefficient of the apparent primitive path quadratic potential $U(L)$. The coefficient ν is obtained by fitting the logarithm of the distribution of primitive path lengths $\ln(P(L))$ to a quadratic function $\nu Z(L/L_{eq} - 1)^2$. The value of ν obtained in this way decreases from around 3 to around 1.5 as r_{tr} increases from 0.0σ to 0.4σ. We also performed simulations of systems with 6016 chains to obtain better statistics. As shown in Figure 1, energy minimization ($r_{tr} = 0$) gives $Z = 5.04 \pm 0.01$ and a quadratic potential with prefactor $\nu = 2.92 \pm 0.10$, while length minimization ($r_{tr} = 0.4\sigma$) yields a slightly smaller value, $Z = 4.91 \pm 0.02$, and a quadratic potential with prefactor 1.57 ± 0.10.

These differences between length and energy minimization can be captured even in a simple two-chain system, shown in Figure 2. In this simple problem, we take the two chains to be orthogonal, before entangling, with one chain of unit length and the other chain of length l, $l \geq 1$. The entanglement point (x, y, z) is then determined by requiring that the chains meet at the entanglement point while either minimizing the total length of the two chains, subject to holding the chain ends fixed at their original positions, which corresponds to a constant tension for each chain, or by minimizing the total energy of the two chains, assuming an energy quadratic in the length of each chain, which corresponds to a chain tension that is linear in the chain length. The coordinates of the two ends of the short chain are fixed at (0, 0, 0) and (1, 0, 0), respectively. The coordinates of the ends of the long chain are (a, b, c) and $(a, b, c - l)$, where a, b, and c are assumed to be uniformly distributed random variables on (0, 1), (0, 1), and (0, l), respectively. Contour length distributions are thus obtained by simple samplings, which are performed numerically. Except for $l = 1.0$, the quadratic energy minimization and length minimization procedures predict almost the same average lengths, with a slightly larger (<2% larger) averaged lengths from energy minimization, shown in Table 2. However, except for $l = 1.0$, the chain contour length distributions, shown by the standard deviations, are quite sensitive to the different minimization procedures, with up to 15% difference between the two. Energy minimization gives a much narrower distribution around the averaged contour length than does length minimization for all length ratios studied here, especially for moderate ratios, $l = 2, 5$. Figure 3 shows the contour length distributions of the two chains obtained by minimizing the total quadratic energy and by minimizing the total length at length ratio $l = 2$. The two peaks correspond to distributions for the short and the long chain. In the energy-minimizing procedure, short chains are stretched more toward the average length of the two chains while long chains shrink their sizes toward the average length; as a result, minimizing energy will give a narrower distribution of contour lengths. A quadratic potential in the chain makes a large length ratio between two entangled chains more unfavorable than does a linear potential, which corresponds to length minimization. As a result, we expect a broader distribution resulting from length minimization than from a quadratic energy minimization.

IV. Discussion

We have found that while the average primitive path length per molecule is not sensitive to the method used to identify primitive paths, the distribution of primitive paths is very sensitive to a change from quadratic energy minimization to total length minimization. While both procedures give us a quadratic form for the potential describing the primitive path distribution, energy minimization gives us a much steeper potential (i.e., narrower distribution of primitive paths) than does length minimization. While this difference does not much affect our understand of reptation, which is dominated by the average length of the primitive paths, it is extremely important for the process of primitive path fluctuations, which dominate the relaxation of branched polymers, such as stars, and is also important in the high-frequency relaxation of linear polymers.[6]

Thus, we would like to be able to determine the "true" distribution of primitive path lengths. This question, and the ambiguity in answering it, arise because the tube model, as currently interpreted, forces us to divide polymer relaxation into two basic contributions, namely (1) that arising from movement of a "test" chain in a "fixed matrix" of constraints imposed by the surrounding chains and (2) that arising from motion of the matrix

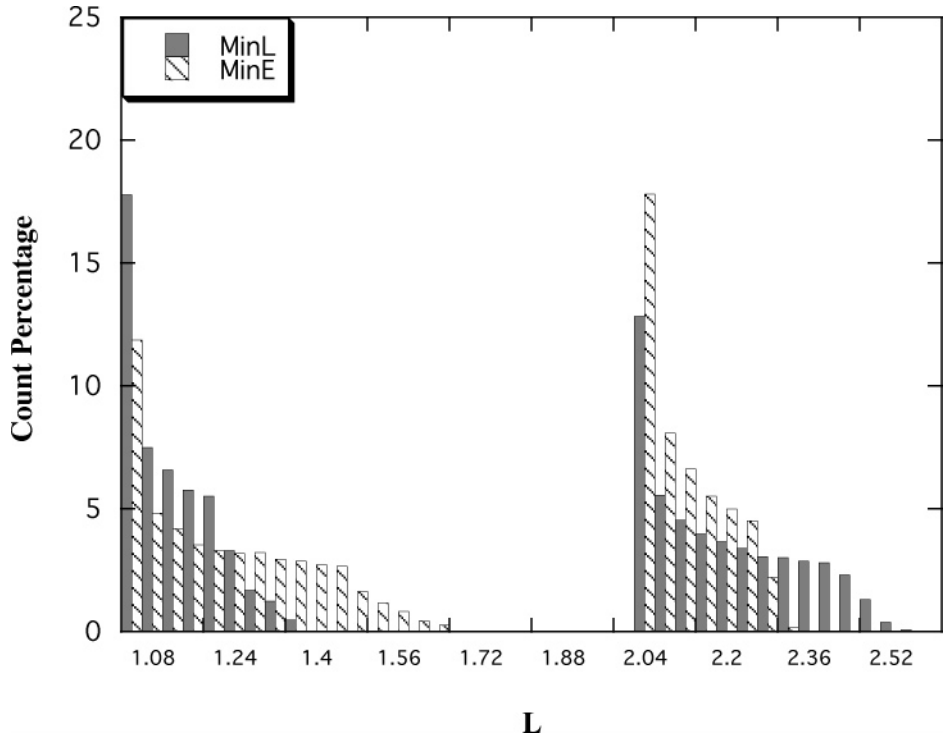

Figure 3. Contour length distributions obtained by minimizing the total quadratic energy and the total length of the two-chain system at length ratio $l = 2$.

Table 2. Average Lengths and Standard Deviations of Length per Chain from Simple Sampling of the Two-Chain System, Depicted in Figure 2, through Length Minimization and Quadratic Energy Minimization

	$l = 1$	$l = 2$	$l = 5$	$l = 10$
length minimization	1.1731 ± 0.0016	1.6337 ± 0.0061	3.0834 ± 0.0229	5.5534 ± 0.0507
std dev	0.1404	0.5493	2.0466	4.5362
energy minimization	1.1731 ± 0.0016	1.6448 ± 0.0052	3.1295 ± 0.0214	5.6248 ± 0.0491
std dev	0.1399	0.4663	1.9114	4.3951

chains. The first of these processes can be analyzed rigorously for simplified models, such as 2-D or 3-D lattice models,[2,14,15] in which, for example, a chain moves on a "pegboard" of fixed obstacles in two dimensions.

If, however, we attempt to identify primitive paths in real space, we encounter the difficulty that while we can insist that the primitive paths we choose satisfy the same topological constraints as the real chains, we can always shorten one "primitive path" by elongating another, and so a method must arbitrarily be chosen to adjudicate the competition between minimizing the lengths of two interlocking primitive paths. We have shown that different choices of how to adjudicate this competition give dramatically different distributions of primitive paths.

In a real melt, the configurations of a single chain and of the network of entanglement constraints around that chain are both dynamic and experience continual fluctuations, at many frequencies. Identification of a fixed set of primitive paths requires suppression of the matrix fluctuations, so that the structure of the real melt is reduced to a form that can be mapped onto the tube model. At root, what makes this step necessary is our need to separate constraint release, which results from the mobility of the matrix and from primitive path fluctuations that occur in a fixed matrix of surrounding topological obstacles.

Given the need artificially to suppress matrix fluctuations to allow separation of motion of the test chain from constraint release produced by the matrix mobility, what is the "best" choice of primitive path? Pragmatically, the "best choice" would presumably be one that allows the tube model to be the most accurate in capturing the relaxation behavior of the real melt. Since the specification of primitive paths artificially suppresses the fluctuations or "breathing" of the matrix structure, it would seem that a choice of primitive paths that allows a broader distribution of their lengths is preferred, since when this is interpreted as a potential, a single chain will then be allowed to explore a broader distribution of primitive path lengths more easily, even within a fixed set of topological restrictions, and this might better capture what happens in real melts, where the mesh of constraints can fluctuate even while preserving topological constraints. This consideration would seem to favor the choice of a minimum total length rather than a minimum quadratic potential. This reasoning is admittedly vague. A more convincing argument might require computing the detailed fluctuations of chains in a melt in which all chain ends are held fixed. A putative method of computing primitive path distributions could then be tested by comparing actual transition rates of chains from one primitive path length to another to that predicted by using the potential derived from the primitive path distribution.

V. Summary

We analyzed the contour length distributions of the primitive paths in large systems of entangled chains. Two methods for identification of primitive paths, namely minimizing the total energy and minimizing the total length, were studied. These two methods give

almost the same average primitive path length per polymer but very different distributions of primitive path lengths. An application of length minimization in primitive path identification yields a quadratic potential for the primitive path distribution with a prefactor ν around 1.5, which is exactly the form proposed by Doi and Edwards[6] and commonly used in modern tube theories to describe relaxation in branched polymers, such as star polymers. Energy minimization also yields a quadratic potential but a quite larger prefactor, $\nu = 3.0$.

Acknowledgment. This work was supported by the NSF under Grant DMR 0305437 and supported by the National Computational Science Alliance under PHY-040025N, utilizing the IBM P690 and the Xeon Linux Supercluster.

References and Notes

(1) Edwards, S. F. *Polymer* **1977**, *9*, 140−143.
(2) Rubinstein, M.; Helfand, E. *J. Chem. Phys.* **1985**, *82*, 2477−2483.
(3) Everaers, R.; Sukumaran, S. K.; Grest, G. S.; Svaneborg, C.; Sivasubramanian, A.; Kremer, K. *Science* **2004**, *303*, 823−826.
(4) Kroger, M.; Ramirez, J.; Ottinger, H. C. *Polymer* **2002**, *43*, 477−487.
(5) Auhl, R.; Everaers, R.; Grest, G. S.; Kremer, K.; Plimpton, S. J. *J. Chem. Phys.* **2003**, *119*, 12718.
(6) Doi, M.; Edwards, S. F. *The Theory of Polymer Dynamics*; Oxford University Press: New York, 1986.
(7) Carmesin, I.; Kremer, K. *Macromolecules* **1988**, *21*, 2819−2823.
(8) Shanbhag, S. A.; Larson, R. G. *Phys. Rev. Lett.* **2005**, *94*, 76001.
(9) Putz, M.; Kremer, K.; Grest, G. S. *Europhys. Lett.* **2000**, *49*, 735−741.
(10) Smith, S. W.; Hall, C. K.; Freeman, B. D. *Phys. Rev. Lett.* **1995**, *75*, 1316−1319.
(11) Smith, S. W.; Hall, C. K.; Freeman, B. D. *J. Chem. Phys.* **1996**, *104*, 5616−5637.
(12) Whittington, S. G. *Topology and Geometry in Polymer Science*; Springer: New York, 1998.
(13) Binder, K. *Monte Carlo and Molecular Dynamics Simulations in Polymer Science*; Oxford University Press: New York, 1995.
(14) Helfand, E.; Pearson, D. S. *J. Chem. Phys.* **1983**, *79*, 2054−2059.
(15) Khokhlov, A. R.; Nechaev, S. K. *Phys. Lett. A* **1985**, *112*, 156−160.

MA050347S